Title: **Explanations for excess EQM Straylight**

CI-No: 151 000

Prepared by:	H. Hartmann	Date:	14.7.06
Checked by:	J. Kroeker, S. Idler		17.07.06
Product Assurance:	R. Stritter		19.07.06
Configuration Control:	W. Wietbrock		19.07.06
Project Management:	Dr. W. Fricke		20/07/06

Distribution: See Distribution List (last page)

Issue	Date	Sheet	Description of Change	Release
Draft			new document	
1	24.04.06		new calculation results and other findings implemented	
2	14.07.06		updated according to new findings	

Table of Contents

1 Introduction

This document discusses the straylight results obtained during the EQM tests.

In HP-2-ASED-TN-0076, 2.69% respectively 5.76% of the telescope straylight are predicted for PACS respectively SPIRE for on ground test (for scattered straylight only, not including diffracted straylight, and independent of wavelength). During the EQM tests, excess straylight was found by PACS (see PACS-ME-TR-059), when compared to these predictions. The excess factors reported by PACS are 46 at 88 µm (i.e. measured 124%) and 26 at 177 µm (i.e. measured 70%). SPIRE also reported excess straylight (SPIRE-RAL-NOT-002688, dated 31/01/06).

Specified for in flight conditions is ≤ 10% of the telescope straylight.

Following these findings, some specific straylight tests have been performed by PACS on EQM in December last year (see PACS-ME-TR-060). Various temperatures and irradiations have been changed in order to find the straylight source.

Also new straylight calculations have been made, with the following important changes compared to calculations in TN-0076:

- Better search strategy.
- Entrance Baffle (ENB) flat aperture deleted, and elongation of ENB cylinder introduced.
- ENB cylinder temperature changed.
- Change of the cryocover mirror BRDF for PACS wavelengths.
- Change of reflectivity of SPIRE input section from 0.05 to 0.95.
- Introduction of 95% reflectivity for the other SPIRE structural surfaces, apart from the input section itself. This was not in the model before.
- Calculation of additional paths and sources not considered before.

For more detailed description of changes see chapter 6

In issue 2 the following new items have been considered:

- Cryocover BRDF for PACS wavelengths now according to TIS measurements on cryocover mirror sample (nominal case and worst case consideration)
- additional consideration of the "cavity path" from HIFI (worst case consideration)

2 EQM straylight tests performed

In order to find the reason for the excess straylight, various thermal emissions have been changed, mainly by changing the temperature of the emitting source, and looking whether the straylight on PACS changes. During this testing the thermal emission from the cryocover as an intended source was suppressed, by cooling the cryocover to below 20 K.

The EQM straylight tests concentrated on items which could be varied easily. In total, four potential sources have been tested.

1. The one open LOU window has been illuminated with a lamp. The other windows are replaced by Al-flanges on EQM and therefore could not be removed for this test. No change in straylight was observed.
2. A cable on the optical bench has been excessively heated by leading a current through it. No change in straylight was observed.
3. In order to exclude, that contamination on the cryocover mirrors lead to excess straylight, the cryocover mirrors have been heated to around 220 K for about 10 minutes. This should remove any water contamination from these mirrors. No change in straylight was observed, after the cryocover mirrors were down to below 20 K again.
   However, it turned out that these cryocover mirrors have been at 220 K for a longer period up to only 3 days before. This is too less time to build a significant contamination layer. An influence of potentially contaminated instrument mirrors, mainly at the instrument entrance, cannot be excluded from this. These mirrors were at low temperatures already several months, and the straylight impact can go with the square of the contamination thickness.
4. The temperature of the Entrance Baffle cylinder was varied. This showed a large effect on straylight. At least half of the straylight can be explained by this. The reason nevertheless is not a higher emission from this source, but a better transport of this straylight by scattering on cryocover mirrors (PACS) and by structural parts of the instruments (SPIRE).
   It should be noted, that in TN-0076 also about half of the straylight is expected from the Entrance Baffle cylinder. The other part mainly comes from the warm CVV.

3 Observed differences compared to calculated straylight in TN-0076

As already mentioned in the introduction, PACS measured a factor of 46 higher straylight at 88 µm and a factor of 26 higher straylight at 177 µm, compared to the calculations for straylight in TN-0076 of 2.69% of the telescope straylight. It must be mentioned, that these 2.69% are scattered straylight only, there is an additional contribution from diffraction, which is treated separately in TN-0076 (chapt. 4.2). It also must be noted that these calculations are for ideal configuration. Misalignments as to be expected might contribute another factor of 1.2 to 1.3 (calculated for the case of a cryocover mirror tilt of 40 arcminutes as an example in TN-0076, page 29).

The values measured by PACS correspond to 124% of the telescope straylight at 88 µm and to 70% of the telescope straylight at 177 µm, whereas the specified value (for in flight conditions) is ≤ 10%.

In relation to the nominal telescope contribution (=100%), the measured total straylight except the cryocover mirrors itself therefore is about 124% at 88 µm and about 70% at 177µm.

SPIRE also reported excess straylight and give some hints where it could come from (SPIRE-RAL-NOT-000, dated 31/01/06). The calculated straylight in TN-0076 here was 5.76% of the telescope straylight.

4 Observed differences EQM-configuration versus straylight model in TN-0076

a) Corrected in AN-0020:

- Entrance Baffle flat aperture is missing in EQM.
- On +X side of Entrance Baffle cylinder there was an elongation made with Al-foil (glued to the baffle cylinder). The elongation in +X direction was about 16 – 18 mm. The gap between CVV bottom and Entrance Baffle cylinder top is 14.5 mm in the model. Therefore this elongation goes somewhat into the CVV hole, but in nominal case does not touch the CVV, because the opening in the CVV has a somewhat larger diameter. The nominal free space is only about 1-2 mm and in reality a slight touching of the warm CVV therefore cannot be totally excluded. The temperature of this elongation could not be determined. From the attachment point of view it should have about the temperature of the Entrance Baffle. However, it turned out that the attachment was not very good. The (worst case) temperature of this elongation therefore is assumed to be in the middle between Entrance Baffle temperature and CVV temperature, which is 180 K. This elongation also covers about the upper 14 mm of the Entrance Baffle cylinder.
- SPIRE surfaces from the entrance plane up to the filter 1 were modelled black, with reflectivity 0.05. It turned out that this entrance section is metallic, with much higher reflectivity, except for a small section of estimated 30 – 50 cm² area. The actual average reflectivity of the entrance section therefore is assumed to be 0.95.
- Temperature of Entrance Baffle cylinder during straylight measurements was higher than expected (67 K instead of 57 K in calculations).

b) not corrected in AN-0020:

- HiFi is modelled with flight configuration. In the EQM, only channel 3 is in flight configuration, the other channels are covered by a tilted Al-plate, which, however, leads some less straylight from the LOU windows into HiFi via other holes. It also could bend more light from the LOU windows towards the path between instruments and Instrument Shield, but this is minor and is covered by the model assumptions.
- Only Thermal Shield 1 was polished internally to have a high reflectivity, whereas the other thermal shields and the Instrument Shield surfaces were untreated surfaces, leading to higher absorption. In terms of straylight this improves the situation slightly, because more straylight is absorbed by them.
- The boundary between PACS and SPIRE cryocover mirrors is slightly curved in the Y-Z-plane. In the model this is approximated by a straight boundary.

c) Already contained in TN-0076:

- During STM straylight inspection a path from the two LOU alignment windows was detected, going sideways along HIFI via the space between instrument shield and instruments towards the detectors. This is considered in this analysis (line "LOU- and alignment-windows via gap between Instrument Shield and instruments" in tables 6.2-1 and 6.2-2), in the same ways as it already was done in the old analysis TN-0076 (Table 4.1-1). It is analysed only in a coarse manner without modelling the detailed instrument configuration for the way from LOU towards the gap between instrument shield and instruments.

5 Further potential impacts not considered in the new straylight model for EQM

- Contamination of the entrance mirrors in both PACS and SPIRE could cause additional scattering not considered in the model. Contrary to the CVV mirrors, which have been heated up to remove contamination, but were at cold temperatures only for a period of 3 days before, the instrument entrance mirrors were at cold temperatures for about 3 months, and therefore could have collected much more water contamination (factor of about 30) than the CVV mirrors. Note also that the straylight effect (TIS) goes with about the square of roughness. If the roughness goes with thickness, then the effect onto straylight could be about a factor of 900 higher for the instrument mirrors. However, PACS also explained that severe contamination would probably cause other effects, which would be noticed by PACS. And SPIRE reported verbally, that it would need very thick contamination to make an effect. So in total this explanation is unlikely.
- The 3rd EQM straylight inspection showed, that some light goes also through the inactivated HiFi channels, but significantly less than through the nominal channel No. 3. In the analysis, the Flight Model HiFi is contained with 7 active channels. This represents a worst case for HiFi.
- The filling port of the Tank is at 300 K. There are small slits in the MLI surrounding this filling port at each feed through of the thermal shields. This could lead some 300 K emission towards the instruments, via paths between Thermal Shield 1 / Instrument Shield and between Instrument Shield / Instruments. However, these slits are small compared to the openings in the LOU baffle, where 300 K emission goes through directly towards the space between Thermal Shield 1 / Instrument Shield and between Instrument Shield / Instruments. This filling port therefore has been neglected. The same apply to the fixation struts between CVV and He-tank.
- Structural surfaces are contained not completely in the models for SPIRE, PACS and HiFi. This makes calculations with reflecting internal structural surfaces questionable to a certain extend, at least for the high reflective surfaces of SPIRE. Note that after the calculation results presented in this AN-0020, SPIRE has updated the SPIRE ASAP model (introduced 3 important internal structural surfaces and deleted another one). This definitively will have impact onto straylight results for SPIRE.
- The contribution from the blank horizontal surface next to the cryocover mirrors has been neglected so far. The reason is that this surface transports much more straylight from other objects than it emits itself. Only the contribution from the tilted black section of the cryocover has been considered therefore.

- The emissivity of surfaces is assumed to be according to Lambertian law. This is not the case for low reflective surfaces. Example of high polished gold surface shows expected low emissivity only for angles up to about 70 – 80° from normal, whereas for grazing angles the emissivity goes to quite high values (see fig. 5.1-1 below).

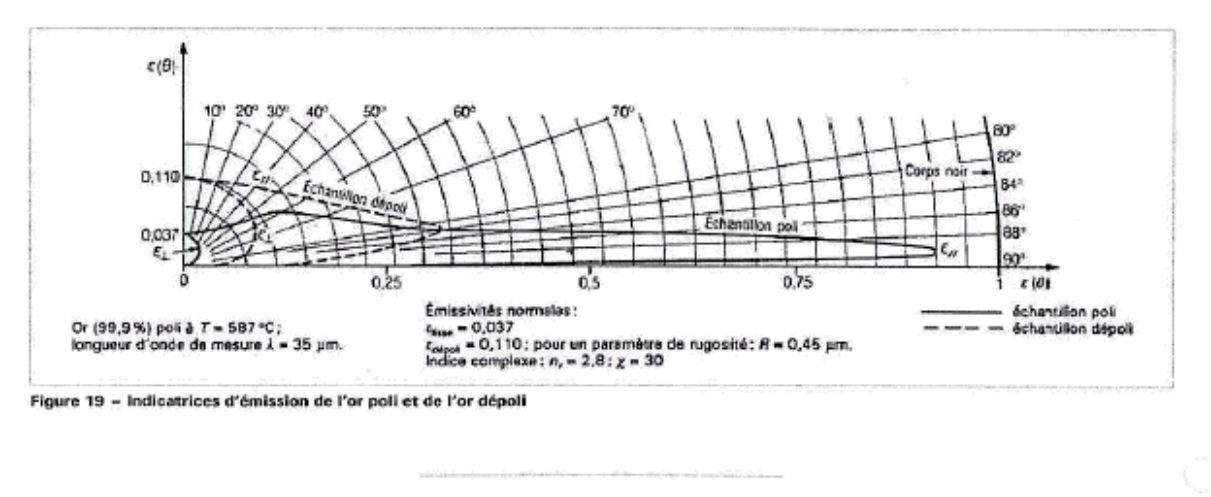

Figure 19 – Indicatrices d'émission de l'or poli et de l'or dépoli

Fig. 5.1-1: Emissivity of gold surfaces as a function of angle against surface normal.

6 New ASAP calculations

6.1 Changes in the model

Due to the large discrepancies, new ASAP calculations have been performed, in order to calculate with more actual design and in order to detect potential calculation errors. The new calculations up to now have been made with the following changes, in order to better reflect the EQM:

- Better search strategy (revealed some additional straylight paths).
- Entrance Baffle flat aperture was deleted, because not in the EQM
- Entrance Baffle cylinder temperature changed from 57 to 67 K.
- Change of the cryocover mirror BRDF for PACS wavelengths. This BRDF now is based on reflectivity measurements performed on the sample for the cryocover mirror, which revealed a somewhat higher BRDF than assumed in the first issue of this AN-0020. For the reflectivity measurement results see figure 6.1-1.

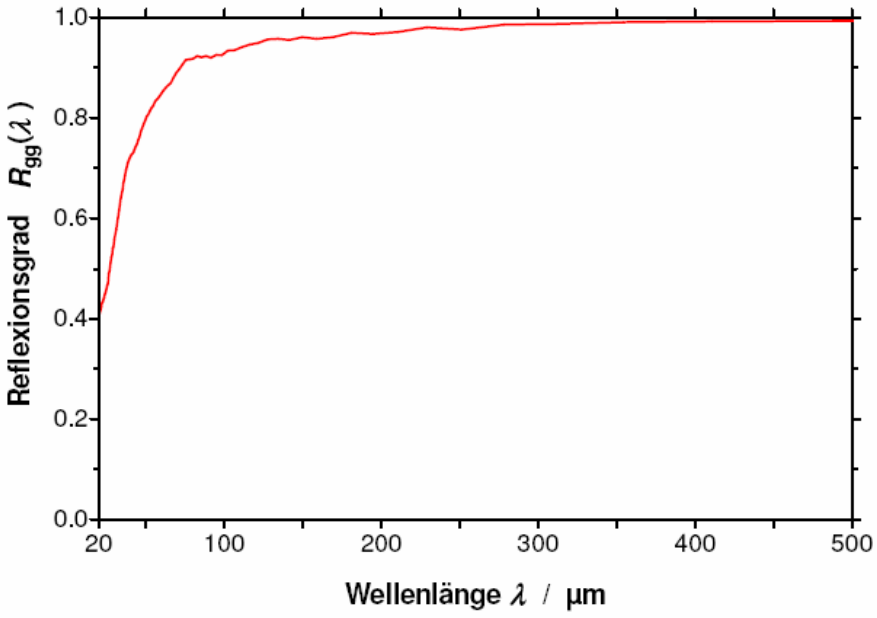

Spektraler Reflexionsgrad $R_{gg}(\lambda)$ der Spiegelprobe unter einem Einfallswinkel von 20° im Wellenlängenbereich von 20 µm bis 500 µm.

Figure 6.1-1 Reflectivity measurement results on cryocover mirror sample

From these reflectivity measurements, TIS (Total Integrated Scatter) values can be derived. In the far infrared, the integral reflectivity (i.e. specular reflectivity plus scatter) of an aluminium surface is very close to 100%. Therefore in first approximation the TIS value is 100% minus specular reflectivity.

Note, however, that nevertheless this remains a high error source in determining the straylight, because only the TIS value could be determined, but not the BRDF itself. Results can vary largely with different slope of the BRDF, even if the TIS of the BRDF remain the same.
These TIS values are

- 8 % +/- 3 % at 88 µm (8% nominal, 11% worst case)
- 3 % +/- 3 % at 177 µm (3% nominal, 6% worst case)

The old BRDF in TN-0076 has a TIS of 0.45 %. To correct this, now the following multiplication factors are used to get the actual EQM BRDF for PACS wavelengths:

Wavelength	Nominal factor	Worst case factor
88 µm	17.8	24.4
177 µm	6.7	13.3

For SPIRE wavelengths such multiplication factors have been neglected in this analysis, because SPIRE EQM is mostly determined by the straylight from reflections at structural walls, and only in negligible amounts from scattering at the cryocover mirror. For STM the cryocover mirror will be polished and will have a much lower BRDF. Further calculations for STM therefore will not use a higher BRDF.

- Introduction of an additional surface with 95% reflectivity / 5% emissivity on the +X side of the ENB cylinder (named "elongation of Entrance Baffle cylinder" in tables 6.2-1 and 6.2-2), covering also the upper 14 mm of the ENB cylinder itself. The temperature of this elongation was assumed to be in the middle between CVV temperature and ENB cylinder temperature, which is quite uncertain. It was attached to the ENB cylinder, but the thermal contact most likely was not very good.
- Change of reflectivity of SPIRE input section from 0.05 to 0.95.
- Introduction of 95% reflectivity for the other SPIRE structural surfaces, apart from the input section itself. This was not in the model before.
- Calculation of additional paths and sources not considered before:
  - Path from LOU windows through HIFI. This now also include an estimate of straylight from a wide angle range ("cavity path"), emitted at the exit of HIFI (near M3). The attenuation inside HIFI was estimated separately without ASAP, based on a worst case reflectivity of 0.998 inside HIFI. This gave a factor 6 reduction between input into and output from HIFI (see HP-2-ASED-FX-0135-06).

- Path from LOU windows towards the gap between Entrance Baffle cylinder and Instrument Shield (previous calculation considered only the path from LOU windows towards the gap between Instrument Shield and Instruments)
- Thermal emission from the gap between Entrance Baffle cylinder and the Instrument Shield cylinder

The following important differences between new model / model geometry and EQM / EQM geometry presently cannot be modelled, at least not in an easy way:

- Thermal emission of white surfaces different from Lambertian law.
- In the model, the cryocover mirror boundary between PACS and SPIRE is a straight line in the Y-Z-plane.

The following differences between new model / model geometry and EQM / EQM geometry are negligible (e.g. against 300 K emission from LOU), and therefore are not in the model:

- Filling port of the Tank
- Fixation struts between CVV and He-tank

Both sources could lead some 300 K emission towards the space between Instrument Shield / Instruments via holes in the Optical Bench, and towards the space between Instrument Shield / Thermal Shield 1, in a similar way as the 300 K emission from LOU windows, but with much less cross sections.

6.2 Results of new calculations

Results are given for two cases, the nominal BRDF and the worst case BRDF. It does affect only the results for PACS. SPIRE therefore is eliminated in the 2nd table.

Emitting object	temperature/ emissivity	PACS detector		SPIRE detector	
		88 µm	177 µm	230 µm	670 µm
CVV ring	295 K / 0.05	3.06	0.59	4.76	3.70
Crown surfaces	293 K / 0.05	2.12	0.40	2.15	1.68
Entrance Baffle (ENB) cylinder	67 K / 0.50	29.78	11.89	85.41	86.77
elongation of ENB cylinder	180 K* / 0.05	1.04	0.15	1.38	1.12
short outer cone of Cryocover	75 K / 0.50	5.67	2.09	17.94	17.53
gap between ENB cylinder and Instrument Shield cylinder	67 K / 0.90	3.72	1.50	3.19	3.24
gap between Instrument Shield and instruments	14 K / 0.90	0.00	0.09	1.34	7.92
Tank via holes in OB	50 K / 0.90	0.65	0.45	2.92	3.38
LOU- and alignment-windows via HiFi (include cavity path worst case)	295 K / 0.90	13.99	2.55	2.79	2.16
LOU- and alignment-windows via gap between ENB cylinder and Instrument Shield cylinder	295 K / 0.90	1.92	0.36	0.66	0.52
LOU- and alignment-windows via gap between Instrument Shield and instruments	295 K / 0.90	1.98	0.42	2.22	1.72
sum scattered light without diffraction / misalignment		**64.1**	**20.6**	**124.8**	**129.7**
additional diffracted light (5 % of scattered light assumed)		3.20	1.03	6.24	6.49
misalignment (30 % of scattered light assumed)		19.24	6.18	37.42	38.92
calculated total		**86.6**	**27.8**	**168.4**	**175.1**
measured during EQM test		**124**	**70**		

Data for PACS and SPIRE are in % with 100% = telescope irradiation (70 K, total ε = 0.03)
* = best estimate only, no destination of temperature possible.
exact measured values during EQM test for SPIRE cannot be given, but also exceed the specification of 10% by more than a factor of 10

Table 6.2-1: Calculated EQM straylight, with nominal BRDF for cryocover mirrors

Emitting object	**temperature/ emissivity**	**PACS detector**	
		88 µm	**177 µm**
CVV ring	295 K / 0.05	4.15	1.11
Crown surfaces	293 K / 0.05	2.89	0.77
Entrance Baffle (ENB) cylinder	67 K / 0.50	40.76	23.41
elongation of ENB cylinder	180 K* / 0.05	1.68	0.51
short outer cone of Cryocover	75 K / 0.50	7.71	3.98
gap between ENB cylinder and Instrument Shield cylinder	67 K / 0.90	5.08	2.93
gap between Instrument Shield and instruments	14 K / 0.90	0.00	0.16
Tank via holes in OB	50 K / 0.90	0.87	0.80
LOU- and alignment-windows via HiFi (include cavity path worst case)	295 K / 0.90	19.16	5.04
LOU- and alignment-windows via gap between ENB cylinder and Instrument Shield cylinder	295 K / 0.90	2.63	0.70
LOU- and alignment-windows via gap between Instrument Shield and instruments	295 K / 0.90	2.66	0.74
sum scattered light without diffraction / misalignment		**87.6**	**40.2**
additional diffracted light (5 % of scattered light assumed)		4.38	2.00
misalignment (30 % of scattered light assumed)		26.28	12.05
calculated total		**118.3**	**54.2**
measured during EQM test		**124**	**70**

Data for PACS are in % with 100% = telescope irradiation (70 K, total ε = 0.03)
* = best estimate only, no destination of temperature possible.

Table 6.2-2: Calculated EQM straylight, with worst case BRDF for cryocover mirrors (PACS only)

Calculations have been performed for scattered light only, with ideal alignment. Additional straylight caused by diffraction and by misalignment then have been added coarsely by certain multiplication factors.

The main differences to the much lower calculation results presented in HP-2-ASED-TN-0076 are due to

PACS: much higher cryocover BRDF

SPIRE: high reflectivity of SPIRE structural surfaces

6.3 Potential explanation of the sharp spot seen in the PACS FOV

In PACS-ME-TR-060 it is reported that there exist an up to now not explained relative sharp straylight spot in the PACS FOV. In the following, it is shown that a larger particle located on the entrance mirror (called TROG1 in the ASAP code) could generate such a spot. It has been investigated with ASAP, how large this potential particle must be, in order to explain the observed feature:

- A small emitting source of 1 mm² area close to TROG1 generates a sharp spot on the detector, via reflection on the cryocover mirror (see Figures 6.3-1 to 6.3-3). The irradiation onto the detector is about 2.5E-3, if the source emits 1 into hemisphere.
- In a second step it was investigated how much irradiation this 1 mm² area gets from the ENB, either directly or via scattering at the cryocover mirror. Result: This 1 mm² receive about 8% of the light which the telescope emits onto the whole detector area, for 88 µm wavelength.

The total result in terms of the usual %age of the telescope emission therefore is 0.02% for 88 µm, which however is concentrated in a small spot on the detector. The spot size in PACS-ME-TR-060 is very roughly estimated by ASED to be about 1/2000 of the detector area (quite uncertain, should be confirmed by PACS, respectively PACS should determine the relative amount of irradiation in this spot compared to the overall straylight in the PACS FOV). If we assume that a 1 mm² particle generates this, then the reflection of light with origin from ENB emission alone would be about 40% of the telescope emission on a 1/2000 fraction of the detector area, exceeding the average level of the straylight from the ENB (25% in Table 6.2-1) locally by about a factor of 1.6.

ASED cannot destine the relative height of the peak in Figure 2 of PACS-ME-TR-060, respectively cannot destine the amount of straylight in this peak relative to the total straylight, because it does not know the zero level.

A photograph taken before the 3rd EQM straylight inspection shows a particle on the PACS entrance mirror (see Fig. 6.3-4).

PACS noted that this peak nevertheless cannot be explained by this mechanism, because it moves twice as fast with chopper angle as the other straylight background, and therefore needs twofold reflection at the chopper.

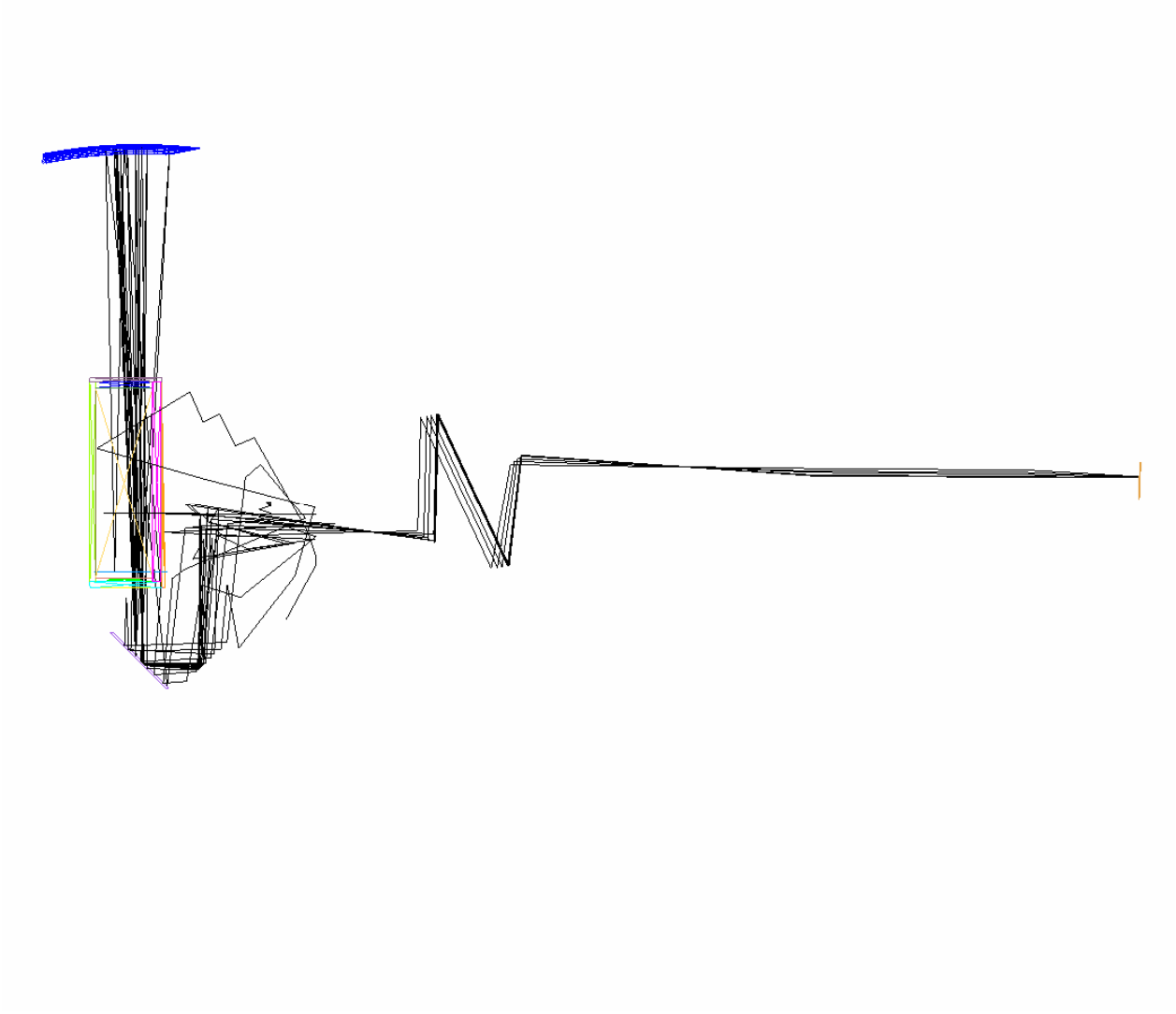

Fig. 6.3-1: General straylight path from particle on TROG1 via cryocover mirror onto PACS detector. For reasons of better visibility of the straylight path only few of the PACS surfaces are shown, and the emitting rays are limited to +/- 5° from normal (not in the real calculation).

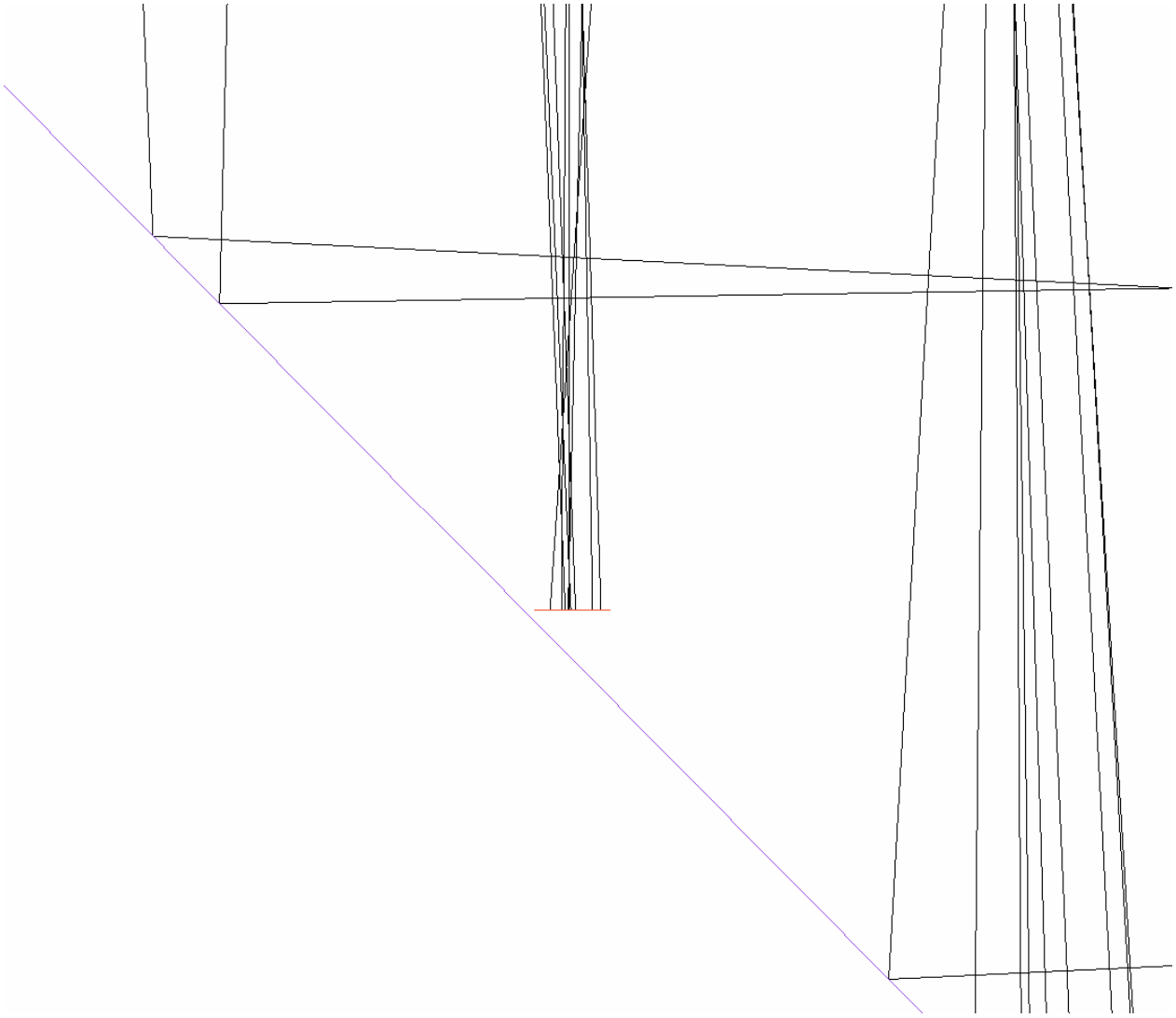

Fig. 6.3-2: Much enlarged cutout of Fig. 6.3-1. Shown are the emitting source (small pink horizontal line) and a section of TROG1 (lilac-coloured tilted line)

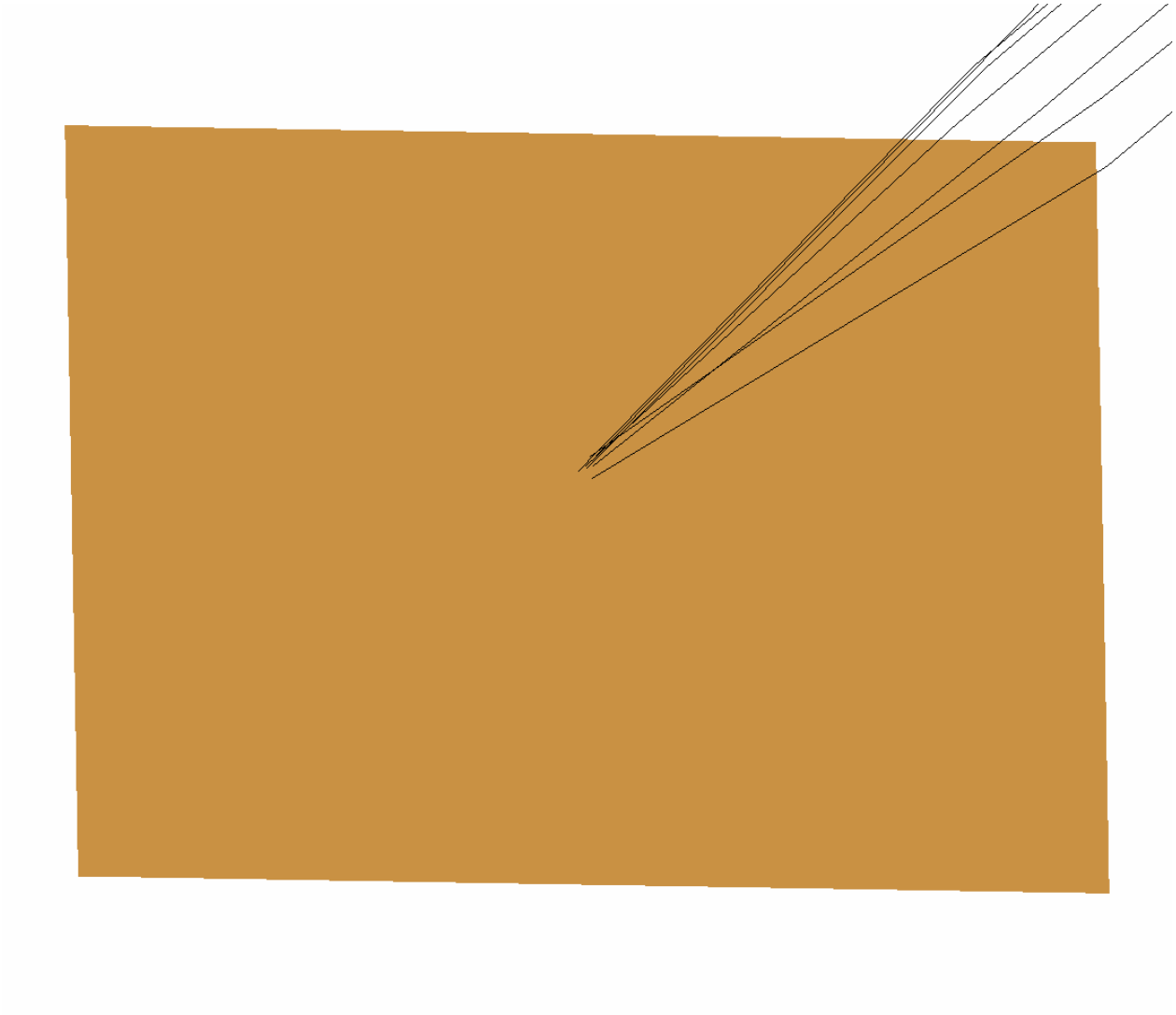

Fig. 6.3-3: Tilted view of the PACS detector, with impinging rays

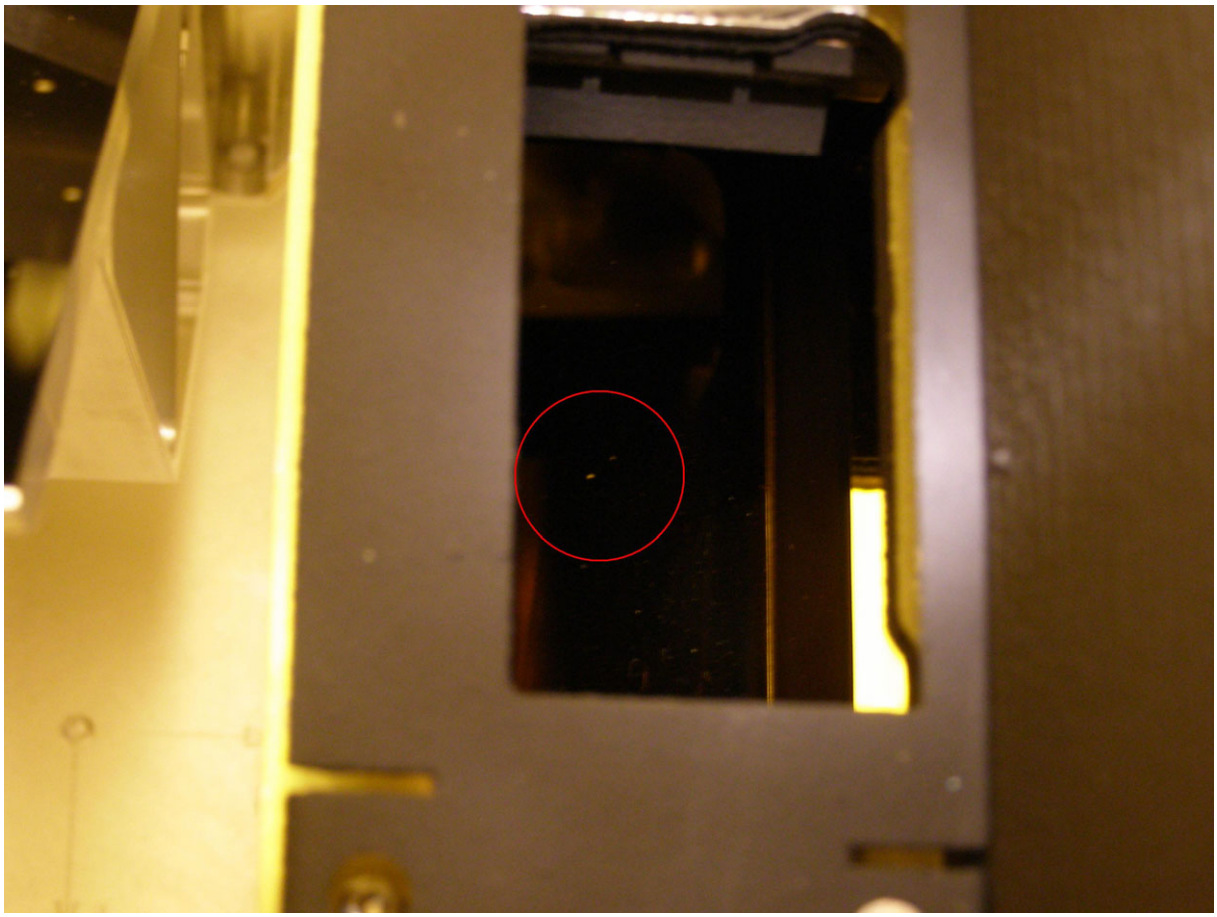

Fig. 6.3-4 Particle on PACS entrance mirror.

7 Summary and expected straylight for STM and FM

7.1 PACS

With the worst case BRDF for the cryocover mirrors, the EQM straylight now nearly is explained. The few % still missing could be explained by

- slope of the BRDF other than assumed
- search strategy missing some minor straylight paths.
- emissivity and reflectivity of surfaces other than assumed.

Provided that the main reason is the different slope of the BRDF, the in flight straylight is expected to be as in TN-0023, because the cryocover mirror then is not in the main straylight path anymore..

Supported is this suspicion by the fact, that the artificial roughness of the cryocover mirror is made such that a larger portion of the microscopic surface seems to be tilted by about 6° against the macroscopic surface (see HP-2-ASED-TR-0038). This also seems to be about the maximum tilt angle. This could cause a much higher BRDF especially at angles around 12° from normal. The question is, whether the long wavelengths still can see this preference in tilting or not. Unfortunately, a BRDF measurement of the cryocover mirror sample was not possible.

If there is significant additional straylight caused by the other reasons mentioned above, then the in flight straylight situation in orbit can be worse, when compared to results in TN-0023. But it still should be much lower than on ground, because most of the on ground straylight is caused by these cryocover mirrors.

The spot like feature seen on EQM will not be present in flight, because it needs the cryocover mirror reflecting back into PACS.

7.2 SPIRE

The most likely reasons for the excess straylight on EQM are reflections at the SPIRE FPU internal structural surfaces. Because the BRDF of the cryocover mirror is much smaller at SPIRE wavelengths, reflection and scattering from this mirror contribute only a small part to the total SPIRE straylight. A drastic reduction for STM and FM will come from the blackening of the input section. Whether this alone already will reduce the straylight to the levels predicted in TN-0023 for FM flight case or whether further SPIRE internal surfaces should be blackened to achieve this is not evident at present.

For STM, the SPIRE straylight is expected to be somewhat higher (coarse estimate only, no ASAP calculation up to now), when compared to results in TN-0076. The value in TN-0076 was 5.76% + factor about 1.3 for diffraction and misalignment, i.e. about 7.5% total. The blackening of the input section may reduce the straylight by an

expected factor of 10 to 20, leaving about 8.5 to 17% of the telescope contribution. The reason mainly will be the reflections on structural walls not considered in the old analysis in TN-0076, but also the improved search strategy and the additional sources considered in this AN-0020 raise the straylight levels somewhat.

8 Actions to reduce straylight for STM and FM

Reduction of straylight for STM and for FM is foreseen by

- Polishing the cryo-cover mirrors for STM and FM (eliminating the artificial cryo-cover micro-roughness). This will reduce the cryo-cover BRDF by more than an order of magnitude and will reduce the PACS straylight for STM and FM on ground quite similar (if it would be measured). In-flight straylight is not affected by this, because the cryocover mirror then will be outside the major light paths. The SPIRE straylight on ground will be not much reduced by this.
- new design (introduction of vanes) of the already existing LOU entrance baffle (LOU TS2 baffle)
- additional LOU TS1 baffle, between LOU TS2 baffle and HIFI FPU
- SPIRE will blacken the SPIRE FPU input section.

The efficiency of the new LOU TS2 baffle together with the new LOU TS1 baffle has been analysed in a comparative manner with ASAP (old design set to 1). The improvement is shown in Figure 8-1. The new baffle design is shown in Fig. 8-2.

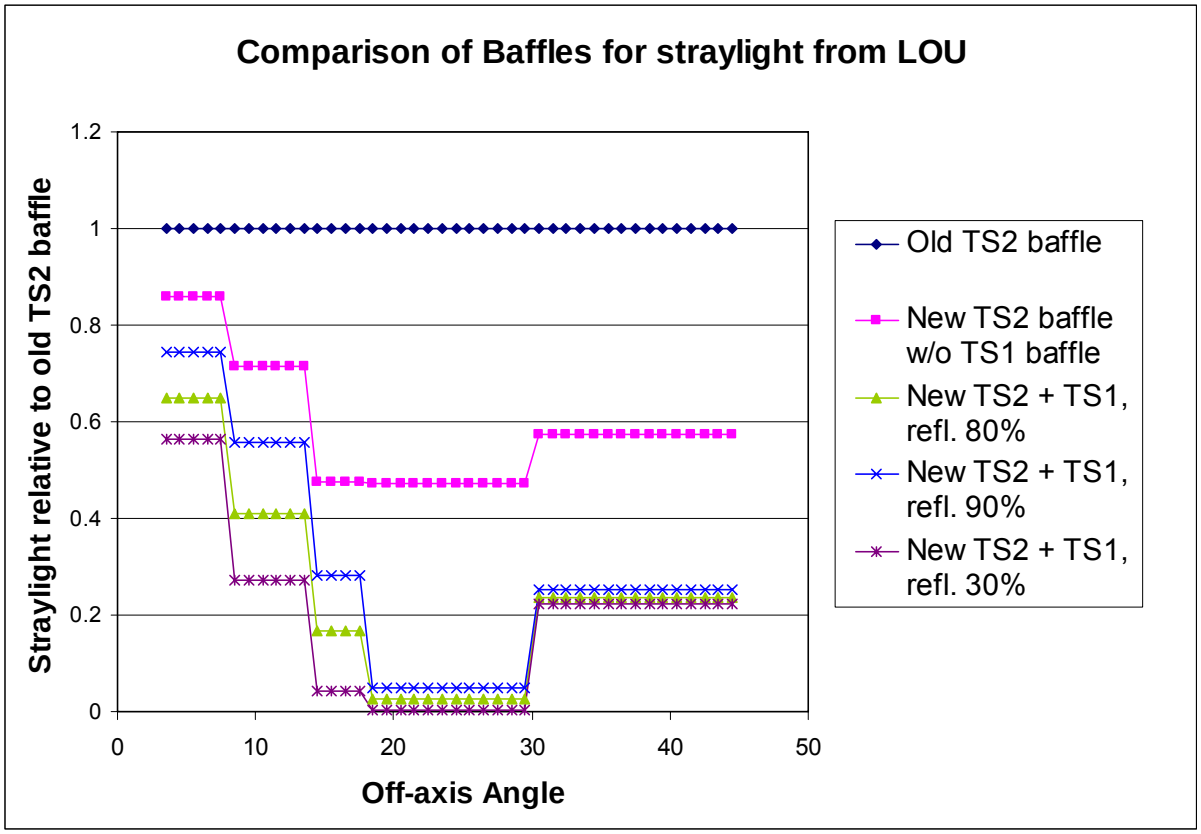

Fig. 8-1: Improvement of straylight from LOU with new baffle design

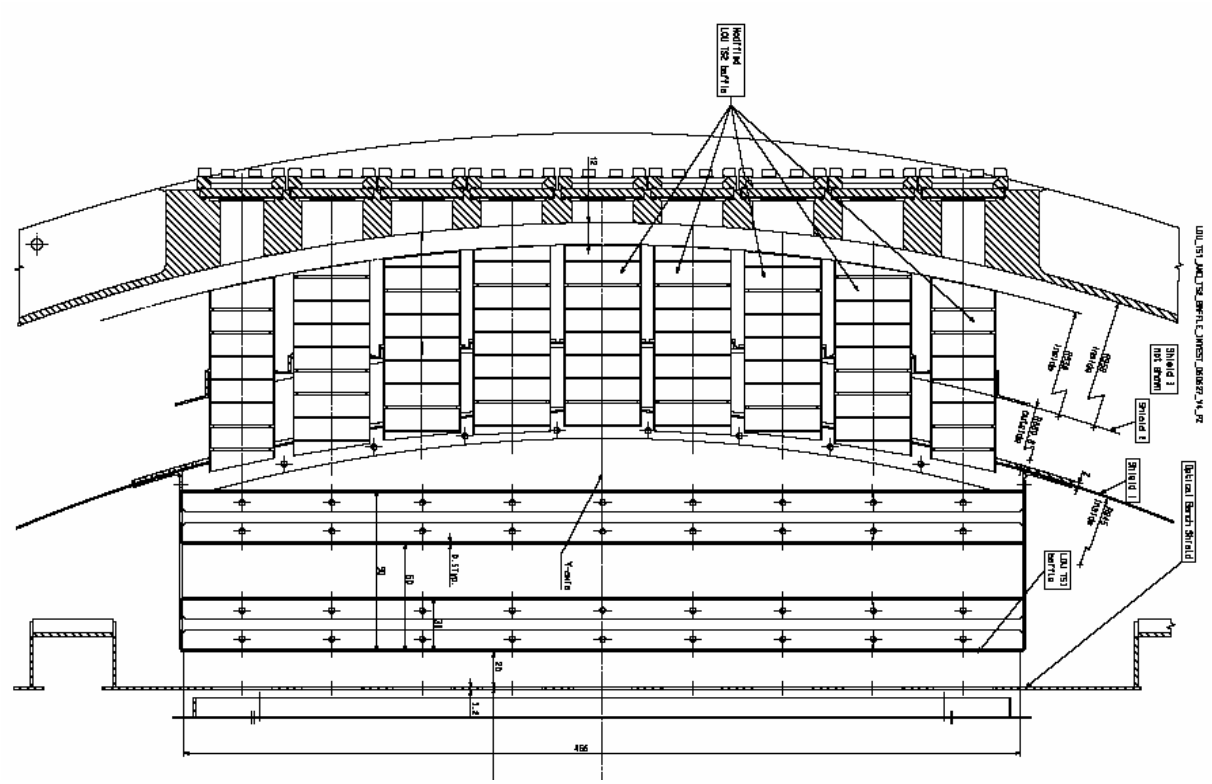

Fig. 8-2: New LOU TS1 and TS2 baffle design

This new baffle design will reduce all 3 paths from LOU in tables 6.2-1 and 6.2-2. Detailed reduction factors for these different contributions have not been computed.

E N D O F D O C U M E N T

	Name	Dep./Comp.		Name	Dep./Comp.
X	Alberti von Mathias Dr.	ASG22		Steininger Eric	AED32
	Barlage Bernhard	AED13	X	Stritter Rene	AED11
	Bayer Thomas	ASA42		Suess Rudi	OTN/ASA44
	Brune Holger	ASA45		Thörmer Klaus-Horst Dr.	OTN/AED65
	Edelhoff Dirk	AED2		Wagner Klaus	ASG22
	Fehringer Alexander	ASG13	X	Wietbrock Walter	AET12
X	Fricke Wolfgang Dr.	AED 65		Wöhler Hans	ASG22
	Geiger Hermann	ASA42		Wössner Ulrich	ASE252
	Grasl Andreas	OTN/ASA44			
	Grasshoff Brigitte	AET12	X	Alcatel Alenia Space Cannes	ASP
X	Hartmann Hans	AED32	X	ESA/ESTEC	ESA
	Hauser Armin	ASG22			
	Hendry David	Terma			
	Hengstler Reinhold	ASA42		**Instruments:**	
	Hinger Jürgen	ASG22	X	MPE (PACS)	MPE
X	Hohn Rüdiger	AED65	X	RAL (SPIRE)	RAL
	Holzle Edgar Dr.	AED32	X	SRON (HIFI)	SRON
	Huber Johann	ASA42		**Subcontractors:**	
	Hund Walter	ASE252		Air Liquide, Space Department	AIR
X	Idler Siegmund	AED312		Air Liquide, Space Department	AIRS
	Ilsen Stijn	Terma		Air Liquide, Orbital System	AIRT
	Iványi von András	FAE12		Alcatel Alenia Space Antwerp	ABSP
	Jahn Gerd Dr.	ASG22		Austrian Aerospace	AAE
	Kalde Clemens	ASM2		Austrian Aerospace	AAEM
	Kameter Rudolf	OTN/ASA42		APCO Technologies S. A.	APCO
	Kettner Bernhard	AET42		Bieri Engineering B. V.	BIER
	Knoblauch August	AET32		BOC Edwards	BOCE
	Koelle Markus	ASA43		Dutch Space Solar Arrays	DSSA
	Koppe Axel	AED312		EADS Astrium Sub-Subsyst. & Equipment	ASSE
X	Kroeker Jürgen	AED65		EADS CASA Espacio	CASA
	La Gioia Valentina	Terma		EADS CASA Espacio	ECAS
	Lamprecht Ernst	OTN/ASQ22		EADS Space Transportation	ASIP
	Lang Jürgen	ASE252		Eurocopter	ECD
	Langenstein Rolf	AED15		European Test Services	ETS
X	Langfermann Michael	ASA41		HTS AG Zürich	HTSZ
	Much Christoph	ASA43		Linde	LIND
	Müller Jörg	ASA42		Patria New Technologies Oy	PANT
	Müller Martin	ASA43		Phoenix, Volkmarsen	PHOE
	Pelz Heinz-Willi	ASG13		Prototech AS	PROT
	Pietroboni Karin	AED65		QMC Instruments Ltd.	QMC
	Platzer Wilhelm	AED2		Rembe, Brilon	REMB
	Reichle Konrad	ASA42		Rosemount Aerospace GmbH	ROSE
	Runge Axel	OTN/ASA44		RYMSA, Radiación y Microondas S.A.	RYM
X	Schink Dietmar	AED32		SENER Ingenieria SA	SEN
X	Schlosser Christian	OTN/ASA44		Stöhr, Königsbrunn	STOE
	Schmidt Rudolf	FAE12		Terma A/S, Herlev	TER
	Schweickert Gunn	ASG22		Terma A/S, Herlev	TERM